Skeletal muscle is enriched in hematopoietic stem cells and not inflammatory cells in cachectic mice

Emanuele Berardi, Paola Aulino, Ivana Murfuni, Angelica Toschi, Fabrizio Padula, Bianca M. Scicchitano, Dario Coletti and Sergio Adamo

Department of Histology and Medical Embryology, Sapienza University of Rome, and Interuniversity Institute of Myology, Via Scarpa, 14 00161 Rome, Italy

Objective: *Cachexia, a debilitating syndrome characterized by skeletal muscle wasting, is associated to many chronic diseases and diminishes the quality of life and survival of patients. Tumor-derived factors and proinflammatory cytokines, including TNF-alpha, IL-6 and IL-1beta, mediate cachexia. In response to elevated cytokine levels, increased proteasome-mediated proteolysis and auto-phagocytosis result in muscle wasting. The histologic features of muscle cachexia are not fully elucidated. Therefore, we analysed alterations of different cell populations in cachectic muscle.*

Methods: *By immunohistochemical and cytological approaches, we characterized changes in the abundance of cellular populations in the musculature of a murine model of cancer cachexia (C26-bearing mice).*

Results: *Cachectic muscle displayed a decreased DNA content proportional to muscle mass wastage. A decrease in the number of nuclei occurred in the muscular but not in the stromal compartment. Cachectic muscle showed: mild modulation of myeloperoxidase activity, a neutrophil marker; reduction of macrophages in the endomysium; decrease in $CD3^+$ lymphocyte number. Conversely, a statistically significant enrichment in $Sca\text{-}1^+CD45^+$ hematopoietic stem cells (HSCs) occurred in cachectic muscle.*

Discussion: *The elevated levels of cytokines which characterize cachexia may represent a trigger for inflammatory cell activation. However, we find that in cachexia, inflammatory cells in muscle are not increased while muscle tissue nuclei decline. Our data suggest that the inflammatory cell-mediated stress is not an etiologic component of muscle wasting in cachexia. The relative increase in HSCs in cachectic skeletal muscle suggests an attempt to maintain muscle homeostasis by recruitment and/or activation of stem cells.* [Neurol Res 2008; **30**: 160–169]

Keywords: Cancer cachexia; hematopoietic stem cells; inflammatory cells; muscle inflammation; muscle injury; muscle wasting

INTRODUCTION

Cachexia is a syndrome characterized by extreme weight loss due to skeletal muscle wasting associated to many chronic diseases, including cancer[1]. Cachexia lowers the patients' responsiveness to therapy contributing to poor prognosis and reducing both quality of life and survival. *In vivo* models of cachexia are based on a chronic, systemic inflammatory state obtained by several approaches including: cytokine gene delivery to a variety of tissues[2,3], recombinant cytokine injection[4] and transplant of tumor cells[5]. Transgenic mouse models developing cachexia include the mice activating NF-κB[6], resulting in muscle wasting and the $Apc^{min/+}$ mice, prematurely developing colon cancer and the associated cachexia[7,8]. Tumor growth and muscle wasting depend on factors of both tumor and host origin, such as tumor necrosis factor α (TNF-α), IL-1β, IL-6, TGF-β, proteolysis-inducing factor and parathyroid hormone-related peptide. These factors lead to muscle wasting through reduced food intake and/or hypermetabolism[9]. Cytokines induce the transcriptional activity of MuRF1 and Atrogin-1/MAFbx which encode E3 ubiquitin ligase proteins mediating degradation of structural and functional muscular proteins[10].

Muscle tissue homeostasis depends not only on the protein synthesis/degradation ratio, but also on the balance between muscle damage and repair. The latter is operated by satellite cells and by stem cells of various origins[11]. Various cell surface markers have been employed to purify adult stem cell populations from skeletal muscle, including CD45, Sca-1, c-kit, CD34[12]. Co-expression of CD45 and Sca-1 characterizes hematopoietic stem cells (HSC) of bone marrow origin, which

Correspondence and reprint requests to: Dario Coletti, Department of Histology and Medical Embryology, Sapienza University of Rome, Via Scarpa, 14 00161 Rome, Italy. [dario.coletti@uniroma1.it] Accepted for publication August 2007.

10.1179/174313208X281046

display myogenic potential[13]. In contrast, Sca-1 and CD45 are not expressed by muscle satellite cells[12,14,15]. In the hindlimb suspension muscle atrophy model, muscle precursor cells have been reported to decrease; the same cells were found to be important for muscle recovery at the end of the atrophying stimulus[16,17]. Changes in cell populations with myogenic potential in cachexia have not been investigated to date.

Cachexia is regarded as associated to a pro-inflammatory environment, due to elevated cytokine levels. Nonetheless, few papers have addressed the interactions between inflammatory cells and skeletal muscle in cachexia. This is of particular relevance, since inflammatory cells may actively participate in the induction of muscle damage and regeneration. In Duchenne's muscular dystrophy, both macrophages and neutrophils have been shown to promote muscle degeneration[18,19]. It is also known that inflammatory cell invasion occurs in acutely damaged skeletal muscle due to toxin injection, lengthening contractions or treadmill exercise[20]. The role of inflammatory cells in muscle damage and healing is complex. For instance, upon acute muscle injury, monocytes are initially recruited to sustain inflammation and shift to an anti-inflammatory role at a later stage to support myogenesis[21]. The importance of favoring the transition from necrosis to regeneration in muscle repair has been recently demonstrated[22]. The immune system cell function in cachexia is still poorly characterized. It has been reported that many tumor-derived cytokines counteract the cytotoxic activity of macrophages and lymphocytes, accounting for the tumor escape from the immune response[23]. Accordingly, several works show structural and functional defects in T lymphocytes that infiltrate tumors[24]. Hampered levels of enzymes involved in antitumor T-cell signal transduction have also been reported[25,26]. Other works showed high levels of apoptosis in T lymphocytes localized both to the tumor mass[27–29] and the lymph nodes[30].

In the present work, we examine whether mononuclear cell number is altered in the musculature of a cancer cachexia model. By analysing different cell populations in the stroma of wasting muscle, we find no evidence of increased presence of inflammatory cells. We also report a significant enrichment in HSC in wasting muscle as compared to controls. Our data indicate that the pro-inflammatory cachectic environment, characterized by elevated cytokine levels, is not sufficient to induce a significant recruitment of inflammatory cells to the musculature. Rather, the same environment may favor stem cell enrichment in muscle as an attempt to maintain muscle homeostasis.

MATERIALS AND METHODS

Animal model of cancer cachexia

Female BALB/c mice, 7 weeks old, were used for this study. To induce cancer-associated cachexia, a 0.5 mm^3 solid fragment of colon carcinoma (C26, obtained from the National Cancer Institute) was subcutaneously implanted in the back of the animals[31]. Treatment of mice was in accordance with the guidelines of the Institutional Animal Care and Use Committee. Several muscles were analysed, depending on the specific experiments (as highlighted in M&M or in the figure legends): the gastrocnemius (GA), the quadriceps femoris (QU), the soleus (SO) and the tibialis anterior (TA).

Histology and histochemistry

The TA was dissected, embedded in tissue freezing medium (Leica, Wetzlar, Germany) and frozen in liquid nitrogen-cooled isopentane. Cryosections (8 μm) were obtained from the midbelly of the muscle using a Leica cryostat (Leica). For histologic analysis, the sections were stained with hematoxylin and eosin (Sigma-Aldrich, St Louis, MO, USA) using standard methods. For NADH-transferase activity, the sections were treated as described by Degenhardt and Sassoon[32].

Esterase staining was adapted from Davis[33] as follows: cryosections of each muscle were incubated for 5 minutes in a staining solution containing: 3 mg α-naphthyl acetate, 0.375 ml acetone, 6.25 ml 0.2M sodium phosphate and 0.4 ml a solution containing equal volumes of 2% pararosaniline (Sigma) and 2% sodium nitrite.

Photomicrographs were obtained using an Axioscop 2 plus system equipped with an Axiocam HRc (Zeiss, Oberkochen, Germany) at standard 1300 × 1030 pixel resolution.

Immunofluorescence analysis

Transverse cryosections were fixed in 4% paraformaldehyde for 10 minutes at room temperature. After incubation with 1% bovine serum albumin (BSA) for 30 minutes, the samples were incubated with a 1 : 100 dilution in BSA of a polyclonal anti-laminin Ab (Sigma), followed by incubation with a 1 : 500 dilution in BSA of anti rabbit-Alexa 568 conjugated Ab (Molecular Probes, Eugene, OR, USA). Nuclei were stained by a 3 minutes incubation with 0.5 μg/ml Hoechst 33342 (Sigma).

Myeloperoxidase assay method

The TA was homogenized in a 1 ml Dounce glass homogenizer containing 0.5 ml of 0.5% hexadecyltrimethylammonium bromide (Kodak) solution in 50 mM potassium-phosphate buffer, pH 6.0 (lysis buffer, LB). Following a 25,000 g centrifugation at 4°C, the supernatant was collected. The pellet was resuspended in 0.5 ml LB and sonicated for 30 seconds. This procedure was repeated three times. The three supernatant fractions were pooled and represented the source of enzymatic activity; 100 μl 2 × reaction solution containing 0.334 mg/ml o-dianisidine dihydrochloride (Sigma) and 0.001% hydrogen peroxide were added to 100 μl of each sample[34]. The colorimetric reaction kinetics was recorded using a Bio-Rad benchmark microplate reader (at a 490 nm wavelength and 37°C). As a positive control, muscle injured 18 hours before the assay by freeze injury was used.

DNA quantification

DNA content was assayed following the method by Labarca and Paigen[35] based on Hoechst 33258 fluorometric intensity readings at a 356/469 Ex/Em wavelength pair. Briefly, chromatin was obtained by sample incubation in a 0.05% Triton X100 in a 20 mM Tris/HCl, 1 mM EDTA and 0.5 M NaCl solution (pH 7.5). Aliquots of the supernatant were incubated with a 0.1 μg/ml Hoechst solution and the fluorescence signal was recorded with a LS50B fluorometer (PerkinElmer, Waltham, MA, USA).

Flow cytometric analysis

The GA was dissected, minced and digested in a solution containing 50 U/ml type II collagenase (Sigma), 35 U/ml type IV hyaluronidase (Sigma) and 1 mg/ml collagenase/dispase in phosphate buffered solution (PBS) for 1 hour at 37°C, to obtain both interstitial and muscle mononuclear cells[36,37]. Following serum addition (to inhibit digestion), the slurry was filtered through a 40 μm strainer, centrifuged and resuspended in PBS. The cells were fixed in 2% paraformaldehyde for 10 minutes, incubated with 1% BSA for 30 minutes, followed by a 1 : 100 dilution in 1% BSA of anti-CD3 monoclonal Ab for 45 minutes (ImmunoTools GmbH, Friesoythe, Germany). The cells were washed and suspended in 0.1% BSA. Analyses were performed on a Coulter Epics XL flow cytometer (Beckman Coulter, Fullerton, CA, USA). Data were analysed with the WinMDI software.

Alternatively, the cells were incubated with a 1 : 200 dilution in 1% BSA of PE-Cy5-conjugated anti-CD45 monoclonal Ab and of FITC-conjugated anti-Sca-1 monoclonal Ab, for 45 minutes at room temperature (BD Biosciences, San Jose, CA, USA). The cells were washed and suspended in 0.1% BSA. Analyses were performed on a Partec PAS III flow cytometer (PARTEC, Muenster, Germany). Data were analysed with the FloMax software.

Morphometric and statistical analysis

Morphometric analysis was performed on type IIb, i.e. low NADH transferase activity, as previously described[3]. For each muscle, average fiber size (cross-section area) was calculated on 200–300 fibers, from a minimum of three randomly chosen fields. To calculate fiber cross-section area, the Scion Image Software was used (a software originally developed with the name of NIH Image at NIH, Bethesda, and freely downloadable at http://www.scioncorp.com/pages/scion_image_windows.htm).

The prevalence of muscular and stromal populations of nuclei in the musculature was evaluated on Adobe Photoshop merged images of laminin and nuclear staining corresponding to a minimum of three randomly chosen fields (including 200–300 cross-sectioned fibers each). The number of nuclei inside and outside the basal lamina was evaluated and normalized by the total fiber number in the corresponding field.

Evaluation of the number of macrophages was performed on a minimum of four randomly chosen fields for each muscle.

All data are expressed as mean ± SD. Statistical analysis was performed by Student's *t*-test using the software available on the VassarStats web page (http://faculty.vassar.edu/lowry/VassarStats.html).

RESULTS

The C26 murine model of cancer cachexia shows severe muscle atrophy

Tumor (C26)-bearing mice are a well established experimental model of cancer-associated cachexia characterized by fast kinetics resulting in the death of the animals within 3 weeks of tumor burden[5,38]. In preliminary experiments, we determined the exponential kinetics of tumor growth following tumor implant (*Figure 1A*) and the associated body weight loss (*Figure 1B*). No significant weight loss was observed until day 17 of tumor load, while tumor-bearing mice had a body weight loss of ~25% compared to control mice by day 21 (*Figure 1B*). NADH-transferase staining was used to discriminate between different fiber type populations and the cross-sectional fast fiber area of the TA was measured as an index of muscle atrophy (*Figure 1C,D*). Tumor-bearing mice showed a shift in fiber size toward smaller dimensions. With this approach, muscle fiber size decline was evident already after 7 days following tumor implant. The atrophic fiber phenotype was confirmed by H&E staining (*Figure 1E*). Atrophy involved most of the fibers, and we did not observ clusters of smaller and irregular myofibers, diagnostic of neurological disorders. In this context, no overt inflammation was observed which would have resulted in a massive infiltration of mononucleated cells. Nonetheless, the density of nuclei appeared higher in cachexia and required further investigation (*Figure 1E*)

Muscle wasting is characterized by loss of muscular but not stromal nuclei

We found a linear correlation between muscle mass and DNA content in various muscles, i.e. SO, TA, QU and GA (*Figure 2A*). We performed the analysis on muscles obtained from control and tumor-bearing animals. As expected, the latter yielded muscle of reduced mass as compared to the matching control muscle, with exception of the SO, a muscle considered more resistant to cachexia (*Figure 2A*). We noticed that the DNA content was also reduced in each cachectic muscle in respect to its control. The linear correlation between muscle mass and DNA content was maintained (*Figure 2A*). Our data suggest that muscle fiber atrophy is associated to loss of muscle nuclei and that an equilibrium is maintained between fiber size and DNA content in cachexia.

We performed an immunohistochemical analysis to discriminate between skeletal muscle fibers and stromal components of the musculature. Laminin staining highlighted the striking fiber atrophy in cachectic mice

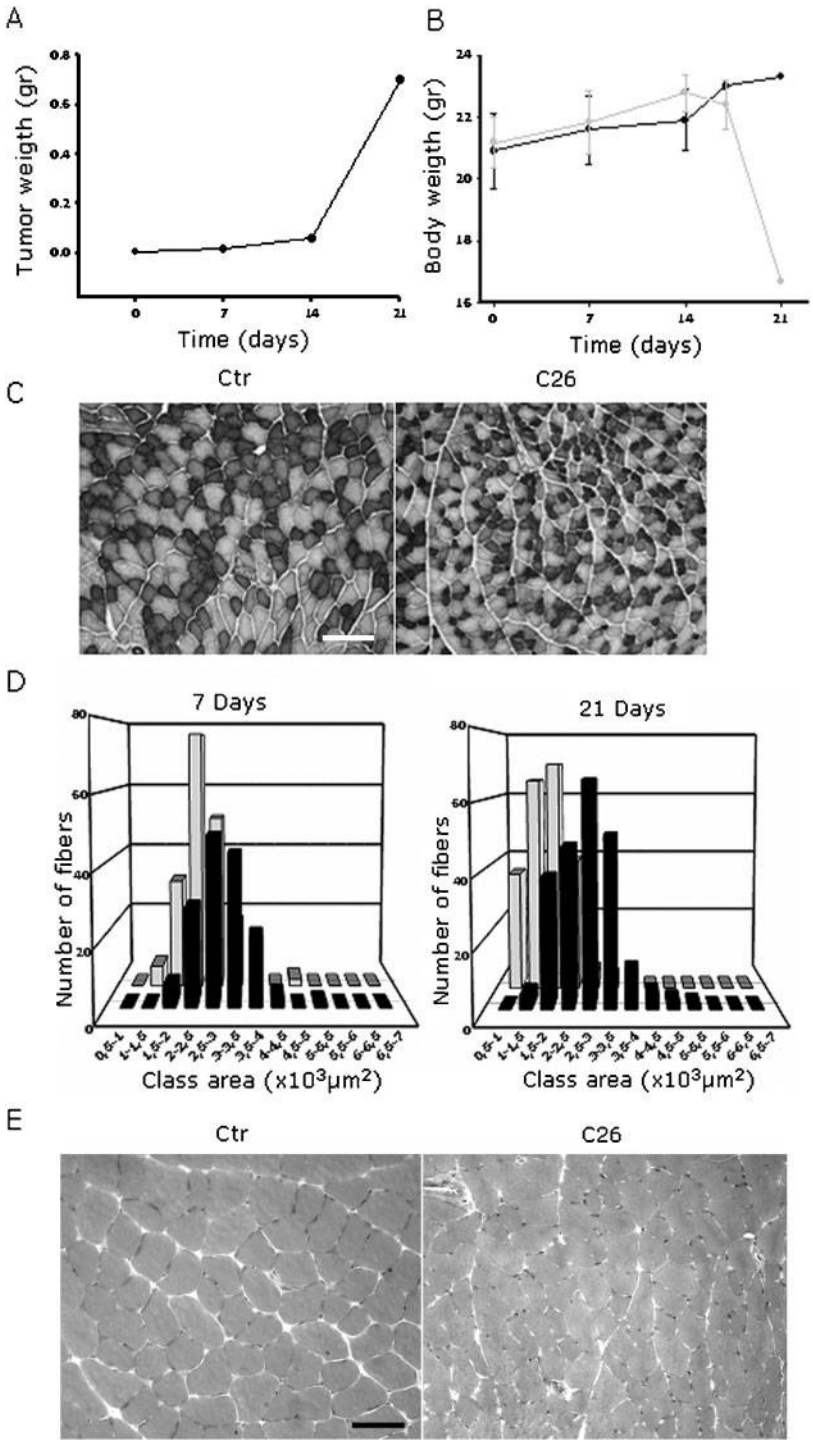

Figure 1: Muscle atrophy is a hallmark of cancer cachexia. (**A**) Time course of tumor growth. C26 tumor was subcutaneously implanted on day 0 (control animals were sham operated). Tumor wet weight at the time of implant or days 7, 14 and 21 is indicated. Following a lag phase, tumor growth is exponential. (**B**) Time course of the carcass weight (body weight). Carcass weight was obtained by subtracting the tumor weight to the animal weight at the time of killing. Tumor-bearing mice displayed a weight loss of ~25% as compared to the control at day 21. (**C**) NADH-transferase histochemistry on muscle transverse cryosections. Representative photomicrographs of TA dissected from control (Ctr) and tumor-bearing mice (C26) on day 21. Cachectic mice displayed muscle fiber atrophy. Bar=100 µm. (**D**) Histograms showing the distribution of the fiber cross-sectional areas in different size classes at days 7 (left panel) and 21 (right panel). Fast fibers of TA from tumor-bearing mice (gray bars) showed a shift of fiber size toward smaller classes of area in cross-section as compared to the control (black bars). (**E**) H&E staining of muscle transverse cryosections. Representative photomicrographs of TA dissected from control (Ctr) and tumor-bearing mice (C26) on day 19. The tumor-bearing animals displayed evident fiber atrophy. No other bulk alterations in the morphology are visible. Bar=50 µm

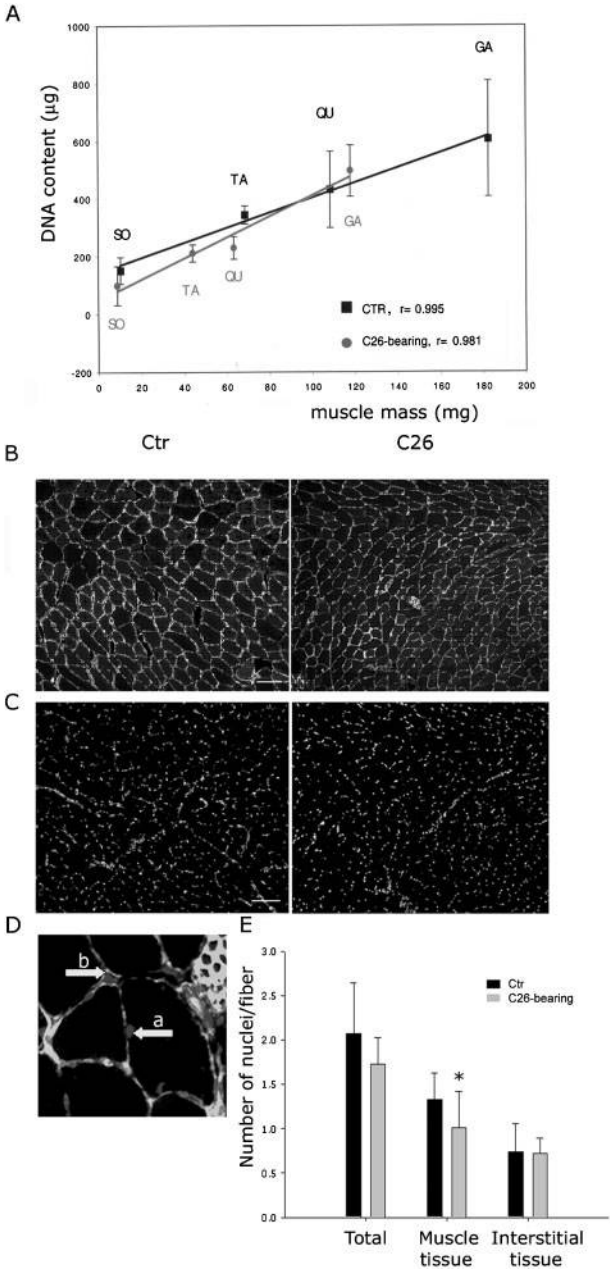

Figure 2: Muscle atrophy is associated to loss of muscle nuclei in cancer cachexia. (**A**) DNA content and muscle mass of different muscles from control (■, CTR) and tumor-bearing (●, C26-bearing) mice on day 19. Data were obtained for the SO, TA, QU and GA, and plotted accordingly to increasing DNA/mass values. The linear correlation factor *r* was calculated for each series of muscles. The mean ± SD of at least three independent experiments is shown. (**B**) Immunofluorescence on transverse cryosections of TA obtained from control (Ctr) and tumor-bearing mice (C26) on day 19. Laminin localization highlights the basal lamina interposed between the skeletal muscle fibers and the stromal compartment. Fiber atrophy is evident in C26-bearing mice. (**C**) Nuclei localized by Hoechst staining in the same microscopic fields as above. Bar=100 µm. (**D**) Merged images at high magnification of the laminin and nuclear staining in a control sample. This approach allows identifying nuclei inside (**a**) and outside (**b**) the basal lamina, i.e. muscle and non-muscle nuclei, respectively. (**E**) Quantitative analysis of photomicrographs of TA obtained from control (Ctr) and tumor-bearing mice (C26) on day 19. At least three randomly chosen microscopic fields per cryosection and three different cryosections (200 µm apart from each other) for each muscle were analysed. Muscle (muscle tissue) and non-muscle nuclei (interstitial tissue) normalized for fiber number (number of nuclei/fiber) were evaluated in control (black bars) and tumor-bearing mice (gray bars). *p=0.050 by Student's *t*-test versus control

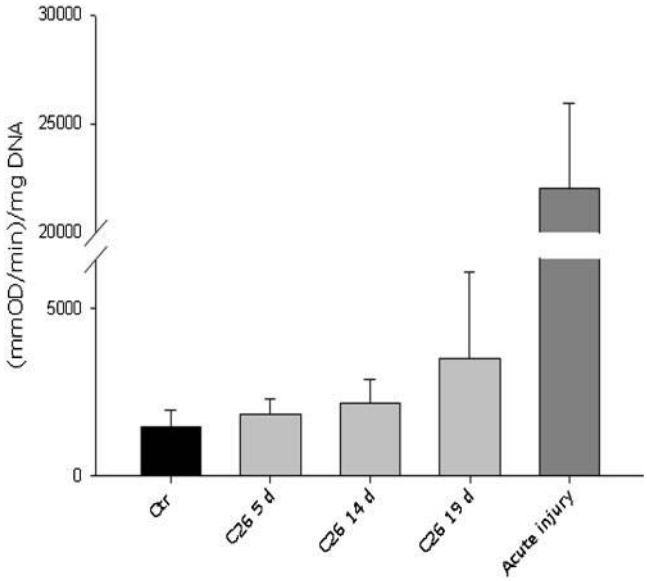

Figure 3: Muscle from tumor-bearing mice exhibits a slight increase in MPO. MPO enzymatic activity in muscle extracts of TA obtained from control (Ctr) and tumor-bearing mice (C26) on various days as indicated. Enzymatic activity (OD/min) was normalized by DNA content. TA collected 18 hours following freeze injury was used as a positive control (acute injury). A mild accumulation of MPO activity was detectable in muscle with the progression of cachexia. The mean ± SD of at least five independent experiments is shown

(*Figure 2B*). Conversely, nuclear staining failed to show any alteration in the quantity and quality of nuclei (i.e. cells) due to cachexia (*Figure 2C*). The numbers of both muscle tissue and non-muscle tissue nuclei were evaluated in muscle cross-sections by counting the nuclei inside and outside the basal lamina on double stained merged images (*Figure 2D*). The total number of nuclei, as well as the number of nuclei outside the basal lamina, was not significantly altered by the presence of the tumor (*Figure 2E*). Cachectic muscle showed a quasi-significant decrease ($p=0.050$ by Student's *t*-test for independent samples with unequal variances) in the number of nuclei underneath the basal lamina, i.e. skeletal muscle tissue.

Myeloperoxidase activity is mildly increased in cachectic muscle

With the aim to analyse in greater detail the activity of non-muscle cells which may be relevant for muscle homeostasis, we used myeloperoxidase activity (MPO) as an indirect measure of neutrophil activity in the musculature. We found that the presence of the tumor induces a mild up-regulation of MPO in the musculature following tumor implant (*Figure 3*). MPO appears several folds lower than what is observed following acute muscle injury, a condition known to produce muscle inflammation and leukocyte invasion, here used as a positive control for the assay.

Macrophage depletion occurs at late stage cachexia

Macrophage number was evaluated by mean of esterase staining on TA muscle cryosections (*Figure 4*). At day 14 following tumor implant, no significant difference was observed in cachectic mice as compared to control mice. Conversely, at day 19 following tumor implant, cachectic muscle displayed a statistically significant decline of macrophage number (*Figure 4D*). The latter time point coincides with the drop in weight loss and is close to the survival limit for tumor-bearing animals. We noted an increase in the esterase signal within the fibers of tumor-bearing animal with time, suggesting accumulation of lysosomes in the wasting fibers (*Figure 4A–C*).

In this context, we also evaluated the number of neuromuscular junctions (*Figure 4A–C*), finding no significant differences in the number of neuromuscular junctions between cachectic and control muscle (data not shown).

Lymphocytes are decreased in cachectic muscle

The GA muscle from either control or tumor-bearing mice was digested with a combination of enzymes to dissociate both fiber-associated and interstitial mononuclear cells[37] and analysed by flow cytometry. To evaluate the relative abundance of lymphocytes, CD3 expression[39] was evaluated in a wide and heterogeneous population of cells gated on the basis of their scatter properties (*Figure 5A*). Tumor-bearing mice displayed a reproducible, even though not significant ($p=0.08$, by Student's *t*-test), decline in the relative abundance of the $CD3^+$ cells present in the musculature as compared to the control, i.e. 16 ± 4.8 and 25 ± 1.4% of the cells, respectively (*Figure 5B,C*). A similar decrease was observed in the number of $CD8^+$ cells (data not shown).

HSCs are increased in cachectic muscle

In a parallel series of experiments, GA muscles from either control or tumor-bearing mice were digested with a combination of enzymes to dissociate both fiber-associated and interstitial mononuclear cells[37] and analysed by flow cytometry. We specifically evaluated the presence in the musculature of Sca-$1^+$$CD45^+$ cells, since this cell population has been shown to possess a significant myogenic potential and to contribute to muscle repair[15]. We found that this cell population represents on average 3.6% of the mononucleated cells in the musculature of control mice, while it is on average 6.5% of the mononucleated cells in the musculature of cachectic mice (*Figure 6A,B*). When expressed as fold increase in respect to the control, the muscular Sca-$1^+$$CD45^+$ population in cachexia displays an almost two-fold, a statistically significant increase in respect to the control ($p<0.05$ by single sample *t*-test). An increase in number was also observed for the Sca-1^+ cells, increased from 6.6% (when the cells are obtained from the musculature of control mice) to 13.2% (when the cells are obtained from the musculature of cachectic mice). No change was observed for the $CD45^+$ cells, which was on average 18% of the mononucleated cells of the muscle examined.

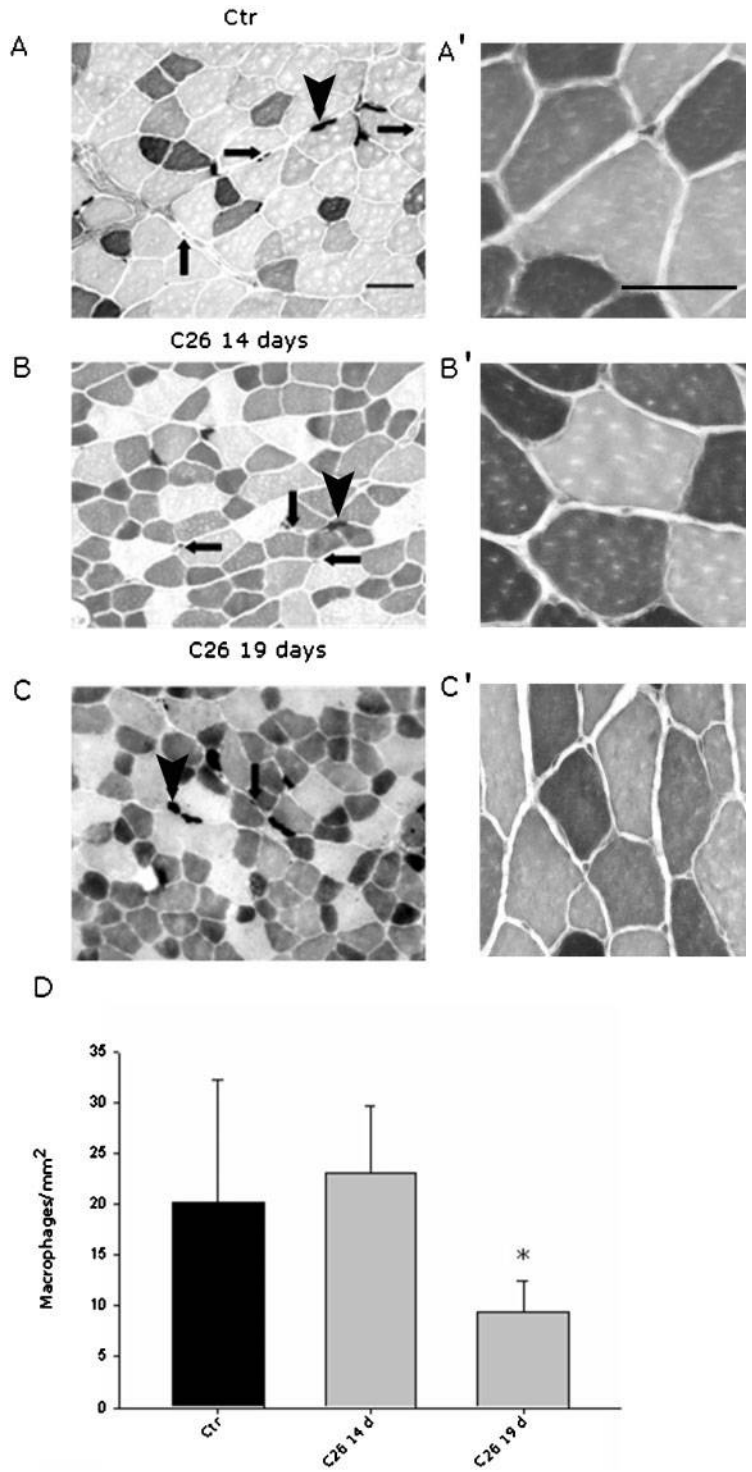

Figure 4: Muscle from tumor-bearing mice shows a biphasic modulation of the macrophage content. Esterase histochemistry on muscle transverse cryosections. (**A**–**C**) Representative photomicrographs of TA dissected from control (Ctr) and tumor-bearing mice (C26) at the indicated time points. The strongest staining is exhibited by neuromuscular junctions (arrowheads) and by macrophages in the endomysium (arrows). A generalized fiber atrophy is not accompanied by a decline in the number of neuromuscular junctions. Bar=25 μm. (**A′**–**C′**) Photomicrographs at higher magnifications of muscle samples as above. Bar=25 μm. (**D**) Macrophage number normalized by surface area was counted and the results shown are expressed as mean ± SD of at least three independent experiments. No differences between control and cachectic mice in the macrophage number at day 14 of tumor load were observed. Macrophages in cachectic muscle declined at day 19. *$p<0.05$ by Student's *t*-test versus control or C26 at day 14

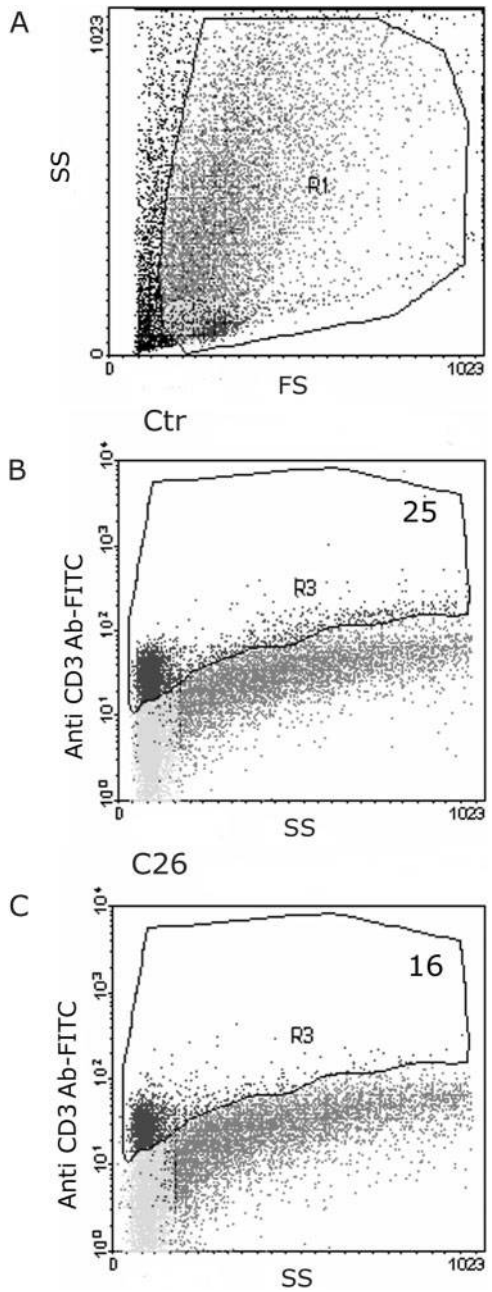

Figure 5: Muscle from tumor-bearing mice is depleted in lymphocytes. Flow cytometric analysis of mononucleated cells obtained by enzymatic digestion of GA from control (**A** and **B**; Ctr) and tumor-bearing mice (**C**; C26) on day 14. (**A**) Forward scatter (FS) versus side scatter (SC) dot plot showing R1 gated cell population of cells used for analysis; (**B** and **C**) SS versus anti-CD3 (anti-CD3 Ab-FICT) dot plot showing $CD3^+$ (R3 gated) and CD3 negative cells. The percentage of $CD3^+$ cells, obtained averaging at least three independent experiments, is indicated. Most of the $CD3^+$ cells are characterized by low SS as expected for lymphocytes. $CD3^+$ cell number is decreased in cachectic muscle

DISCUSSION

Cachexia is widely regarded as secondary to a condition of chronic inflammation due to the elevated levels of pro-inflammatory cytokines in the circulation of patients and animal models[40]. Chronic inflammation often promotes aggressive tumor growth and spread[41]. Inflammatory cytokines also induce activation and scattering of inflammatory cells and the general perception exists that inflammatory cells are increased in cachexia. However, very few data are available on the inflammatory cell response in cachexia. In two different rat models of cancer cachexia, an overall immunosuppression has been actually reported[30,42]. In particular, Vannucci *et al*. report a significant decrease in circulating NK, B and T lymphocytes in tumor-bearing animals[42]. de Lima *et al*. show apoptosis in peripheral lymphocytes of tumor-bearing animals, a phenomenon which may account for the decrease in circulating lymphocytes[30]. To our knowledge, the only report on leukocyte populations infiltrating the musculature of cachectic animals is the observation by Acharyya *et al*. that no statistically significant differences in the number of lymphocytes or macrophages occurred as compared to controls[38]. We investigated in detail the presence of inflammatory cells in the musculature of C26-bearing mice at several time points after tumor load, by quantifying neutrophils, macrophages and lymphocytes (*Figures 3–5*). None of these cell populations accumulates in muscle in the course of cachexia. On the contrary, we observed a non-significant decline in the number of lymphocytes and an abrupt decline in macrophages at the late stage of cachexia. Accumulation of neutrophils and macrophages in murine skeletal muscle following chronic TNF-α administration has been reported[43]. However, the latter does not represent a model of cachexia, since TNF-α treated mice do not display the hallmarks of muscle wasting[43]. Our data are in agreement with previous observations on *in vivo* models of muscle wasting and extend to the murine model of cachexia the findings obtained in rats[30,42]. Our observation that inflammatory cells do not increase in cachectic muscle is relevant in the light of the influence inflammatory cells have on muscle homeostasis. Indeed, inflammatory processes are very important in muscle injury and repair. Inflammation is regarded as a useful response to damage necessary to trigger muscle regeneration. However, it is important to distinguish between features of muscle inflammation that promote injury and those that promote repair. The multiple roles played by neutrophils and macrophages in muscle injury and repair have been recently reviewed by Tidball[44]. Both neutrophils and macrophages might contribute to muscle wasting in cachexia by inducing muscle damage and/or by a paracrine action based on released cytokines. Our data strongly suggest that these cell populations are not responsible for muscle damage in cachexia.

The contribution of HSC to muscle homeostasis has been reported[45] even though its relevance in steady state conditions is still debated. In contrast, HSC recruitment and myogenic conversion are stimulated by muscle injury or other insults[45]. By flow cytometry of cells extracted from control and cachectic muscles, we evaluated the presence of Sca-1^+ $CD45^+$ cells, a population with myogenic potential[14]. We found that these stem cells are doubled in the musculature of

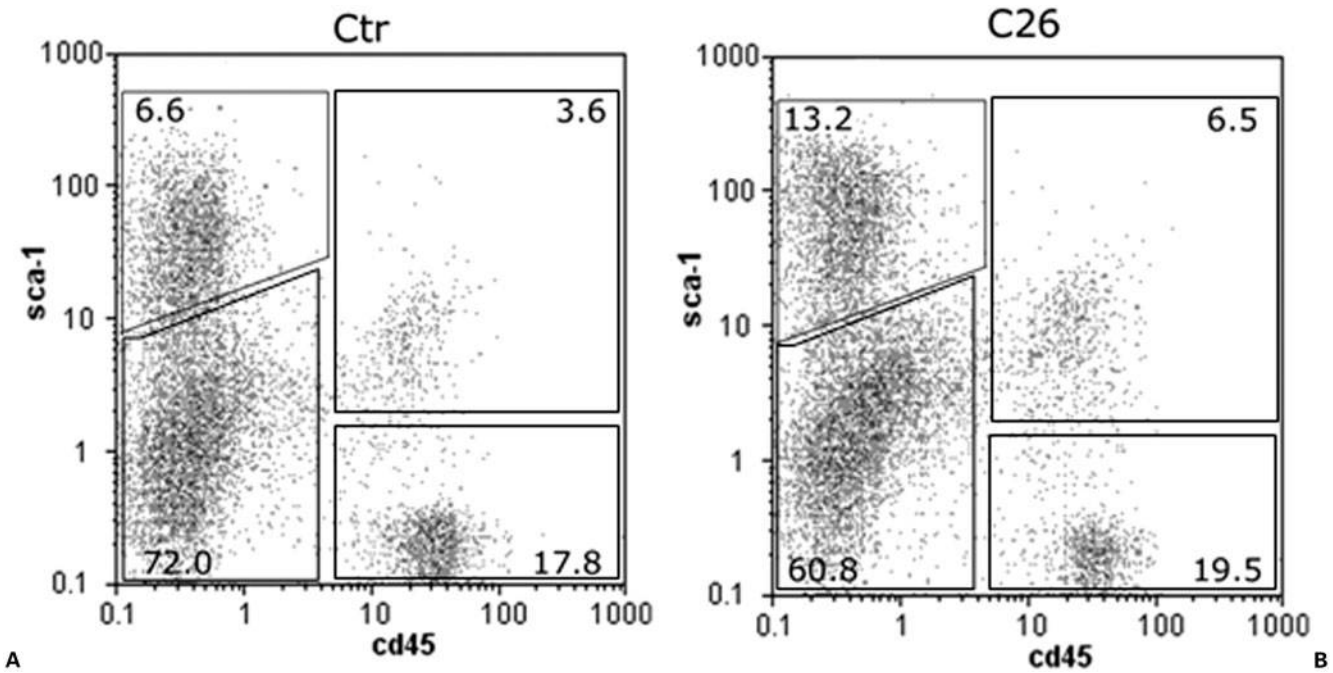

Figure 6: Muscle from tumor-bearing mice is enriched in HSC. Flow cytometric analysis of mononucleated cells obtained by enzymatic digestion of GA from control (Ctr, **A**) and tumor-bearing mice (C26, **B**) on day 19. Anti-CD45 (CD45) versus anti-Sca-1 (Sca-1) dot plots are divided in regions to evaluate the number of cells positive for each antigen. The percentage of cells for each region, obtained averaging at least three independent experiments, is indicated. Cachectic muscle are specifically enriched in Sca-1$^+$CD45$^+$ cells in respect to the control

cachectic mice (*Figure 6*), in contrast with other cell populations of bone marrow origin. We interpret this phenomenon as a response to signals released by the atrophying fibers. HSC do not appear to be sufficient to maintain muscle homeostasis, and muscle wasting still occurs, suggesting that HSC function or survival is hampered in cachexia. HSC intervention may result in an abortive attempt to regenerate wasting muscle. The mechanisms underlying this phenomenon are under investigation.

Another non-muscle tissue which is fundamental for the maintenance of muscle fiber trophism is the nervous tissues. The histopathologic features of neurological disorders, i.e. clusters of smaller and irregular myofibers, were not observed in cachectic muscles (*Figure 1*). In addition, we did not observe a decline in the number of neuromuscular junctions, suggesting that survival of motor neurons is not hampered in cachexia (*Figure 4* and data not shown). Therefore, we propose that the motor neuron degeneration is not involved in the muscle wasting observed in cachexia.

Losses of both myonuclei and muscle precursor cells have been reported in hind limb suspension[17]. The relevance of these findings stems from the fact that muscle precursor cells are important for muscle recovery at the end of the atrophying stimulus[16]. In the present paper, we demonstrate a loss of nuclei specifically affecting the skeletal muscle tissue in a much more severe condition of muscle wasting than unloading (*Figure 2*). Muscle nuclei are the majority of the nuclei found in any cross-section and their decline in cachexia may account for the decrease in both total nuclear number and DNA content we observe in cachexia. We also show a strong linear correlation between muscle mass and DNA content of the musculature, which is maintained in the shift from physiologic to pathologic conditions (*Figure 2*). It is not known whether in cachexia the loss of muscle nuclei precedes or follows fiber cytoplasm reduction. Still, this observation contributes to the knowledge about adaptations of the 'nuclear domains' in skeletal muscle fibers. It has been recently shown that aging is accompanied by a drop in fiber nuclear number[46]. A model is proposed whereby the inability of muscle nuclei to support an excessive domain size over time leads to cytoplasmic atrophy; the latter restores a fixed nuclear domain size and leads to the atrophic morphology typical of aged muscle[46]. In cachexia, the drop in the number of nuclei associated to each fiber suggests the occurrence of apoptosis. Indeed, apoptosis has been reported in skeletal muscle of patients with chronic diseases frequently associated to cachexia[47,48].

ACKNOLEDGEMENTS

This work was funded by AFM (project no. 11788-SR) and Progetti di Ateneo of Sapienza University of Rome (to S. Adamo). The technical expertise of Ms C. Ramina and the scientific inputs of Dr A. Pristerà are gratefully acknowledged.

REFERENCES

1 Tisdale MJ. Molecular pathways leading to cancer cachexia. *Physiology (Bethesda)* 2005; **20**: 340–348

2 Oliff A, Defeo-Jones D, Boyer M, *et al.* Tumors secreting human TNF/cachectin induce cachexia in mice. *Cell* 1987; **50**: 555–563
3 Coletti D, Moresi V, Adamo S, *et al.* Tumor necrosis factor-alpha gene transfer induces cachexia and inhibits muscle regeneration. *Genesis* 2005; **43**: 120–128
4 Guttridge DC, Mayo MW, Madrid LV, *et al.* NF-kappaB-induced loss of MyoD messenger RNA: Possible role in muscle decay and cachexia. *Science* 2000; **289**: 2363–2366
5 Schwarzkopf M, Coletti D, Sassoon D, *et al.* Muscle cachexia is regulated by a p53-PW1/Peg3-dependent pathway. *Genes Dev* 2006; **20**: 3440–3452
6 Cai D, Frantz JD, Tawa NE, Jr, *et al.* IKKbeta/NF-kappaB activation causes severe muscle wasting in mice. *Cell* 2004; **119**: 285–298
7 Groden J, Thliveris A, Samowitz W, *et al.* Identification and characterization of the familial adenomatous polyposis coli gene. *Cell* 1991; **66**: 589–600
8 Mehl KA, Davis JM, Berger FG, *et al.* Myofiber degeneration/regeneration is induced in the cachectic ApcMin/+ mouse. *J Appl Physiol* 2005; **99**: 2379–2387
9 DeJong CH, Busquets S, Moses AG, *et al.* Systemic inflammation correlates with increased expression of skeletal muscle ubiquitin but not uncoupling proteins in cancer cachexia. *Oncol Rep* 2005; **14**: 257–263
10 Acharyya S, Guttridge DC. Cancer cachexia signaling pathways continue to emerge yet much still points to the proteasome. *Clin Cancer Res* 2007; **13**: 1356–1361
11 Peault B, Rudnicki M, Torrente Y, *et al.* Stem and progenitor cells in skeletal muscle development, maintenance, and therapy. *Mol Ther* 2007; **15**: 867–877
12 Asakura A, Seale P, Girgis-Gabardo A, *et al.* Myogenic specification of side population cells in skeletal muscle. *J Cell Biol* 2002; **159**: 123–134
13 Rivier F, Alkan O, Flint AF, *et al.* Role of bone marrow cell trafficking in replenishing skeletal muscle SP and MP cell populations. *J Cell Sci* 2004; **117**: 1979–1988
14 Polesskaya A, Seale P, Rudnicki MA. Wnt signaling induces the myogenic specification of resident $CD45^+$ adult stem cells during muscle regeneration. *Cell* 2003; **113**: 841–852
15 Seale P, Ishibashi J, Scime A, *et al.* Pax7 is necessary and sufficient for the myogenic specification of $CD45^+$:$Sca1^+$ stem cells from injured muscle. *PLoS Biol* 2004; **2**: E130
16 Mitchell PO, Pavlath GK. A muscle precursor cell-dependent pathway contributes to muscle growth after atrophy. *Am J Physiol Cell Physiol* 2001; **281**: C1706–C1715
17 Mitchell PO, Pavlath GK. Skeletal muscle atrophy leads to loss and dysfunction of muscle precursor cells. *Am J Physiol Cell Physiol* 2004; **287**: C1753–C1762
18 Acharyya S, Villalta SA, Bakkar N, *et al.* Interplay of IKK/NF-kappaB signaling in macrophages and myofibers promotes muscle degeneration in Duchenne muscular dystrophy. *J Clin Invest* 2007; **117**: 889–901
19 Hodgetts S, Radley H, Davies M, *et al.* Reduced necrosis of dystrophic muscle by depletion of host neutrophils, or blocking TNFalpha function with Etanercept in mdx mice. *Neuromuscul Disord* 2006; **16**: 591–602
20 Pizza FX, Peterson JM, Baas JH, *et al.* Neutrophils contribute to muscle injury and impair its resolution after lengthening contractions in mice. *J Physiol* 2005; **562**: 899–913
21 Arnold L, Henry A, Poron F, *et al.* Inflammatory monocytes recruited after skeletal muscle injury switch into antiinflammatory macrophages to support myogenesis. *J Exp Med* 2007; **204**: 1057–1069.
22 Pelosi L, Giacinti C, Nardis C, *et al.* Local expression of IGF-1 accelerates muscle regeneration by rapidly modulating inflammatory cytokines and chemokines. *FASEB J* 2007; **21**: 1393–1402
23 Elgert KD, Alleva DG, Mullins DW. Tumor-induced immune dysfunction: The macrophage connection. *J Leukoc Biol* 1998; **64**: 275–290
24 Prins RM, Graf MR, Merchant RE. Cytotoxic T cells infiltrating a glioma express an aberrant phenotype that is associated with decreased function and apoptosis. *Cancer Immunol Immunother* 2001; **50**: 285–292
25 Radoja S, Frey AB. Cancer-induced defective cytotoxic T lymphocyte effector function: Another mechanism how antigenic tumors escape immune-mediated killing. *Mol Med* 2000; **6**: 465–479
26 Whiteside TL. Signaling defects in T lymphocytes of patients with malignancy. *Cancer Immunol Immunother* 1999; **48**: 346–352
27 Chappell DB, Restifo NP. T cell-tumor cell: A fatal interaction? *Cancer Immunol Immunother* 1998; **47**: 65–71
28 Gastman BR, Johnson DE, Whiteside TL, *et al.* Tumor-induced apoptosis of T lymphocytes: Elucidation of intracellular apoptotic events. *Blood* 2000; **95**: 2015–2023
29 Rivoltini L, Carrabba M, Huber V, *et al.* Immunity to cancer: Attack and escape in T lymphocyte-tumor cell interaction. *Immunol Rev* 2002; **188**: 97–113
30 de Lima TM, Lima MM, Almeida DC, *et al.* Cachexia induced by Walker 256 tumor growth causes rat lymphocyte death. *Cancer Immunol Immunother* 2005; **54**: 179–186
31 Tanaka Y, Eda H, Tanaka T, *et al.* Experimental cancer cachexia induced by transplantable colon 26 adenocarcinoma in mice. *Cancer Res* 1990; **50**: 2290–2295
32 Degenhardt K, Sassoon DA. A role for Engrailed-2 in determination of skeletal muscle physiologic properties. *Dev Biol* 2001; **231**: 175–189
33 Davis BJ. Histochemical demonstration of erythrocyte esterases. *Proc Soc Exp Biol Med* 1959; **101**: 90–93
34 Rubin BB, Smith A, Liauw S, *et al.* Complement activation and white cell sequestration in postischemic skeletal muscle. *Am J Physiol* 1990; **259**: H525–H531
35 Labarca C, Paigen K. A simple, rapid, and sensitive DNA assay procedure. *Anal Biochem* 1980; **102**: 344–352
36 Rando TA, Blau HM. Primary mouse myoblast purification, characterization, and transplantation for cell-mediated gene therapy. *J Cell Biol* 1994; **125**: 1275–1287
37 Sherwood RI, Christensen JL, Conboy IM, *et al.* Isolation of adult mouse myogenic progenitors: Functional heterogeneity of cells within and engrafting skeletal muscle. *Cell* 2004; **119**: 543–554
38 Acharyya S, Butchbach ME, Sahenk Z, *et al.* Dystrophin glycoprotein complex dysfunction: A regulatory link between muscular dystrophy and cancer cachexia. *Cancer Cell* 2005; **8**: 421–432
39 Fujihashi K, Kiyono H, Aicher WK, *et al.* Immunoregulatory function of $CD3^+$, $CD4^-$, and $CD8^-$ T cells. Gamma delta T cell receptor-positive T cells from nude mice abrogate oral tolerance. *J Immunol* 1989; **143**: 3415–3422
40 Barton BE. IL-6-like cytokines and cancer cachexia: Consequences of chronic inflammation. *Immunol Res* 2001; **23**: 41–58
41 MacDonald N. Cancer cachexia and targeting chronic inflammation: A unified approach to cancer treatment and palliative/supportive care. *J Support Oncol* 2007; **5**: 157–162
42 Vannucci L, Fiserova A, Horvath O, *et al.* Cancer evolution and immunity in a rat colorectal carcinogenesis model. *Int J Oncol* 2004; **25**: 973–981
43 Peterson JM, Feeback KD, Baas JH, *et al.* Tumor necrosis factor-alpha promotes the accumulation of neutrophils and macrophages in skeletal muscle. *J Appl Physiol* 2006; **101**: 1394–1399
44 Tidball JG. Inflammatory processes in muscle injury and repair. *Am J Physiol Regul Integr Comp Physiol* 2005; **288**: R345–R353
45 Sherwood RI, Christensen JL, Weissman IL, *et al.* Determinants of skeletal muscle contributions from circulating cells, bone marrow cells, and hematopoietic stem cells. *Stem Cells* 2004; **22**: 1292–1304
46 Brack AS, Bildsoe H, Hughes SM. Evidence that satellite cell decrement contributes to preferential decline in nuclear number from large fibres during murine age-related muscle atrophy. *J Cell Sci* 2005; **118**: 4813–4821
47 Vescovo G, Zennaro R, Sandri M, *et al.* Apoptosis of skeletal muscle myofibers and interstitial cells in experimental heart failure. *J Mol Cell Cardiol* 1998; **30**: 2449–2459
48 Vescovo G, Volterrani M, Zennaro R, *et al.* Apoptosis in the skeletal muscle of patients with heart failure: Investigation of clinical and biochemical changes. *Heart* 2000; **84**: 431–437